Electronic Supplementary Information

Influence of hydrogen bonds and π-π stacking on the self-assembly of aryldipyrrolidones

Pedro Ximenis,[a] Llorenç Rubert,[a] Heike M. A. Ehmann[b] and Bartolome Soberats*[a]

[a] Department of Chemistry, University of the Balearic Islands, Cra. Valldemossa, Km. 7.5, Palma de Mallorca, Spain.

[b] Anton Paar GmbH, Anton-Paar-Straβe 20, 8054 Graz, Austria.

Table of Contents

1. Experimental methods

Nuclear Magnetic Resonance Spectroscopy: NMR spectra were recorded o an Advance (300 mHz) from Bruker at 298 K. The spectra were calibrated using the residual protic solvent as internal standard and the chemical shifts (δ) were recorded in parts per million (ppm). For temperature-dependent experiments, a temperature control system was used in heating mode.

Mass spectrometry: ESI-HRMS mass spectra were measured in Thermo Scientific Orbitrap Q Exactive mass spectrometer equipped with electrospray modules.

Matrix-assisted laser desorption/ionization-time of flight (MALDI-TOF) mass spectrometry (MS): MALDI-TOF spectra were measured a MALDI-TOF BRUKER Autoflex III Smartbeam mass spectrometer equipped with Smartbeam laser technology.

Ultraviolet-Visible Spectroscopy: The measurements in solution were carried out with Jasco V-750 UV-vis spectrometer in quartz glass cuvettes (Hellma) using spectroscopic grade chloroform (99%+ stabilized with amilene) and methylcyclohexane (99%) from ACROS and tetrahydrofuran (99.6% stabilized with BHT) from Thermoscientific. The solid-state experiments were measured with Agilent Cary 5000 UV-Vis-NIR equipped with Diffuse Reflectance accessory (DRA-2500) using 1.25 mm quartz round plates (Hellma).

Atomic Force Microscopy: AFM images were taken with a Veeco NanoScope IV MultiMode (Veeco, Santa Barbara, CA) using tapping mode.

Infrared Spectroscopy: The measurements in solid state of Fourier transform infrared-attenuated total reflection (FTIR) spectra were recorded on a Bruker Tensor 27. The spectra were recorded over a range of 400−4000 cm^{-1} and an average of 16 scans was taken for each spectrum. The experiments in solution were carried out in a Bruker Vertex 80V IR spectrometer in CaF_2 glasses using spectroscopic grade chloroform (99%+ stabilized with amilene) and deuterated methylcyclohexane (>99.5%) from Euroisotop. The spectra were recorded over a range of 400−4000 cm^{-1} and an average of 16 scans was taken for each spectrum.

Fluorescence spectroscopy: Fluorescence excitation-emission spectra were recorded on a Cary Eclypse spectrophotometer. The measurements were carried out in quartz glass cuvettes (Hellma) using spectroscopic grade chloroform (99%+stabilized with amilene) and methyl cyclohexane (99%) from ACROS. Slit widths were set to 10 mm bandpass for both excitation and emission. All spectra were recorded at 25 ± 1 °C.

Wide angle X-ray scattering (WAXS): WAXS data were recorded on a laboratory SAXS beamline (SAXSpoint 5.0, Anton Paar, Graz, Austria) equipped with a Primux 100 micro X-ray source (Anton Paar, Graz, Austria) and a 2D EIGER2 R 1M hybrid photon counting detector (Dectris). The scattering patterns were measured with 300 s exposure time in gapless mode (detector was shifted in height and a second exposure was recorded to fill the gap) at ambient conditions. A range of momentum transfer of $0.03 < s < 1.46$ $Å^{-1}$ was

covered ($s = 4\pi \sin(\theta)/\lambda$, where 2θ is the scattering angle, and λ is the X-ray wavelength, in this case 1.542 Å). The data processing was done using the SAXSanalysis package (Anton Paar, version 4.50).

Differential Scanning Calorimetry: DSC measurements were carried out was carried out with a Mettler Toledo DSC 3+. The data given for the thermal transitions were obtained from the second heating and first cooling scans.

Polarizing Optical Microscopy: POM images were obtained with a Flexacam C1 attached to a Leica DM2700P microscope equipped with a Linkam LTS420 hot stage or with a Axiocam 208 color camera attached to a Axio Imager.A2 microscope by Zeiss with a Linkam LTS420 heating stage.

2. Synthetic procedures

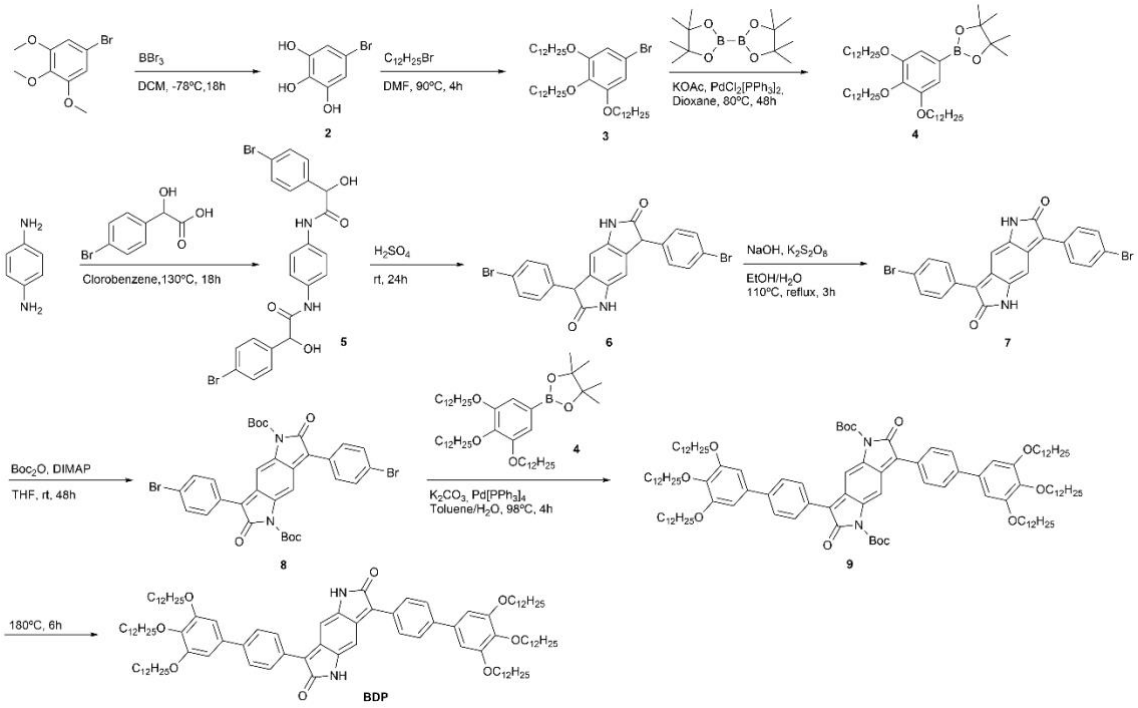

Fig. S1. Synthetic scheme of **BDP**.

Compound **4** was synthetized according to reference S1. Compounds **7** and **8** were prepared according to references S2 and S3 respectively.

*Compound **9***

50 mg (0.07 mmol) of compound **8**, 163 mg (0.22 mmol) of compound **4** and 8 mg (0.0072 mmol) of $Pd[PPh_3]_4$ were introduced in a dried Schlenk and were degassed for 20 min. Meanwhile, 20 mL of toluene were also degassed, and then 10 mL were introduced in the Schlenk, the mixture was again degassed for 20 min. Finally, 10 mL of 5M aqueous solution of potassium hydroxide (KOH) was degassed for 20 min and 5 mL of it were introduced in the Schlenk. The reaction mixture was stirred at 90°C for 5 hours in dark. A dark intense pink solid is formed, and the product is extracted with chloroform (3 x 50 mL), then the organic phase filtered through celite, giving a pink coloured solution. Then, the filtered organic phase is dried with anhydrous sodium sulphate, filtrated and the solvent was evaporated to yield the crude product. The solid was purified by silica-gel flash chromatography using dichloromethane: methanol (100:00 to 90:10 v:v) as eluent to yield the final product as a pink solid (25 mg, 0.01 mmol, 15.5%). The purity of the compound was assessed by ^{1}H NMR and then used with no further purification for the next step.

^{1}H NMR (300 MHz, 298 K, $CDCl_3$) δ (ppm): δ 7.78 (d, J=7.7 Hz, 4H, Ar-H), 7.67 (d, J=7.7 Hz, 4H, Ar-H), 6.81 (s, 2H, Ar-H), 4.08-3.99 (m, 12H, -CH_2-O), 1.87-1.75 (m, 12H, -CH_2-), 1.67 (s, 18H, Boc), 1.51-1.44 m (m, 12H, -CH_2-), 1.26 (m, 96H, -$(CH_2)_8$-), 0.88 (t, J=6.6 Hz, 18H, -CH_3)

BDP

25 mg (0.01 mmol) of compound **9** were dissolved in 5 mL of DCM and the solvent was slowly evaporated to create a film in the rounded-bottom flask. Then the thermal deprotection of Boc was performed by heating the flask at 180°C for 6 hours in dark. The resulting solid was dissolved in 1-2 mL of dichloromethane and then precipitated with methanol. The pure product was obtained as a dark pink viscous solid (10 mg, 0.006 mmol, 62.7%) after a GPC chromatography in chloroform.

^{1}H NMR (300 MHz, 298 K, $CDCl_3$) δ (ppm): 7.78 (d, J=7.8 Hz, 4H, Ar-H), 7.66 (d, J=8.1 Hz, 4H, Ar-H), 7.00 (s, 2H, N-H), 6.80 (s, 4H, Ar-H), 6.57 (s, 2H; Ar-H), 4.07-4.01 (m, 12H, -CH_2-O), 1.86 – 1.79 (m, 12H, -CH_2-), 1.51 – 1.47 (m, 12H, -CH_2-), 1.27 (m, 96H, -$(CH_2)_8$-), 0.88 (t, J = 6.6 Hz, 18H, -CH_3).
^{13}C NMR (75 MHz, 298 K, $CDCl_3$) δ (ppm): 179.43, 154.66, 143.49, 142.43, 139.74, 136.69, 134.22, 131.04, 128.98, 128.57, 107.19, 74.80, 70.53, 36.60, 33.10, 30.84, 27.32, 23.86, 15.28.
HRMS-ESI (+) for $C_{106}H_{166}N_2O_8$ $[MH]^+_{calc}$ = 1596.27; $[MH]^+_{exp}$ = 1596.28

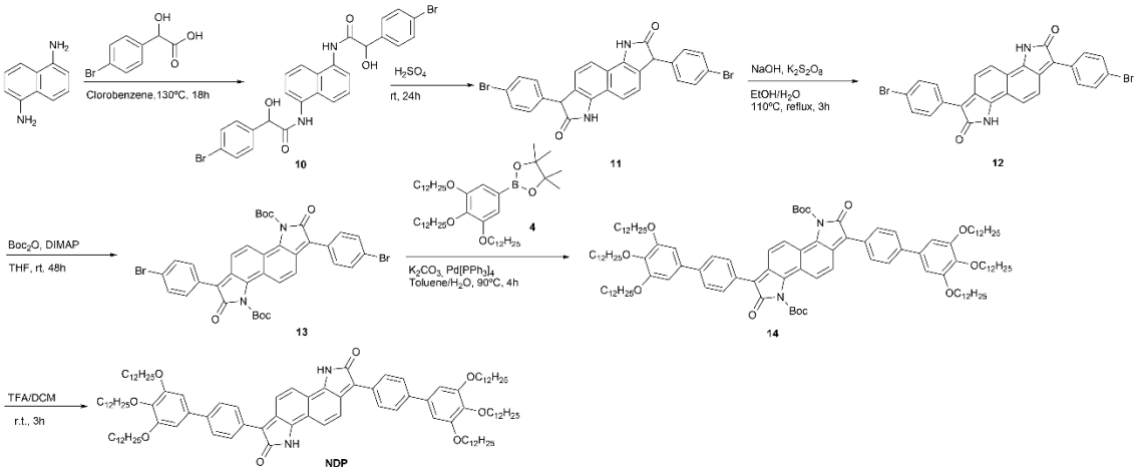

Fig. S2. Synthetic scheme of **NDP**.

Compounds **12** and **13** were prepared according to references S2 and S3, respectively.

*Compound **14***

79 mg (0.11 mmol) of compound **12**, 200 mg (0.26 mmol) of compound **4** and 12 mg (0.011 mmol) of $Pd[PPh_3]_4$ were introduced in a dried Schlenk and degassed for 20 min. Meanwhile, 20 mL of toluene were also degassed, and then 15 mL were introduced in the Schlenk, the mixture was again degassed for 20 min. Finally, 15 mL of 5M aqueous solution of KOH was degassed for 20 min and 10 mL of it were introduced in the Schlenk. The reaction mixture was stirred at 100°C under reflux for 5 hours in dark. A blue intense suspension was formed, and the product was extracted with chloroform (3 x 50 mL). The organic phase was filtered through celite, giving a blue coloured solution. The solution was dried with anhydrous sodium sulphate, filtrated and the solvent evaporated under vacuum. The crude product was dissolved in a small quantity of THF then precipitated by adding hexane. The solid was filtered and dried under vacuum. The pure product was obtained as a blue solid (32 mg, 0.017 mmol, 15.7%) and was used in the next step with no further purification.

^{1}H NMR (300 MHz, 298 K, $CDCl_3$) δ (ppm): 7.78 (d, J=7.7 Hz, 4H, Ar-H), 7.67 (d, J=7.7 Hz, 4H, Ar-H), 6.81 (s, 2H, Ar-H), 4.08-3.99 (m, 12H, -CH_2-O), 1.87-1.75 (m, 12H, -CH_2-), 1.67 (s, 18H, Boc), 1.51-1.44 m (m, 12H, -CH_2-), 1.26 (m, 96H, -$(CH_2)_8$-), 0.88 (t, J=6.6 Hz, 18H, -CH_3)

NDP

15 mg (0.0081 mmol) of compound **14** were dissolved in a round-bottom flask with 2 mL of dichloromethane and the solution was cooled down to 0°C. Then, 2 mL of trifluoroacetic acid were dissolved in 1 mL of dichloromethane and they were slowly added to the cold solution. Then the mixture was stirred at room temperature for 3 hours. 10 mL of a saturated solution of Na_2CO_3 were added to quench the remaining trifluoroacetic acid (this operation generates some bubbles) until pH=8. Then the product was extracted with DCM (3 x 20 mL), the organic phase was dried with anhydrous sodium sulphate, filtered and the solvent evaporated under vacuum. The

crude product was purified by silica-gel flash chromatography using Hexane: THF (95:05 to 25:75 v:v) as eluent. The pure compound was obtained by precipitation in THF/MeOH as a blue solid (7 mg, 0.004 mmol, 52.5%).

^{1}H NMR (300 MHz, THF-*d8*) δ (ppm): 8.00 (d, *J* = 8.2 Hz, 4H, Ar-H), 7.68 (d, *J* = 8.3 Hz, 4H, Ar-H), 7.44 (d, *J* = 9.4 Hz, 2H, Ar-H), 7.26 (d, *J* = 9.5 Hz, 2H, Ar-H), 6.90 (s, 4H, Ar-H), 4.08-3.95 (m, 12H, -CH_2-O), 1.84 – 1.72 (m, 12H, -CH_2-), 1.50 (m, 12H, -CH_2-), 1,28 (m, 96H, -$(CH_2)_8$-), 0.88 (t, J = 6.6 Hz, 18H, -CH_3).
^{13}C NMR (75 MHz, 298 K, THF-*d8*) δ (ppm): 170.47, 154.37, 152.49, 137.98, 136.24, 133.97, 132.23, 130.32, 128.64, 127.45, 125.71, 113.26, 106.48, 73.50, 69.67, 34.91, 32.72, 30.54, 23.39, 21.19, 14.27.
MALDI-TOF for $C_{110}H_{168}N_2O_8$ $[MH]^+_{calc}$ = 1646.33; $[MH]^+_{exp}$ = 1646.28.

3. NMR Spectra

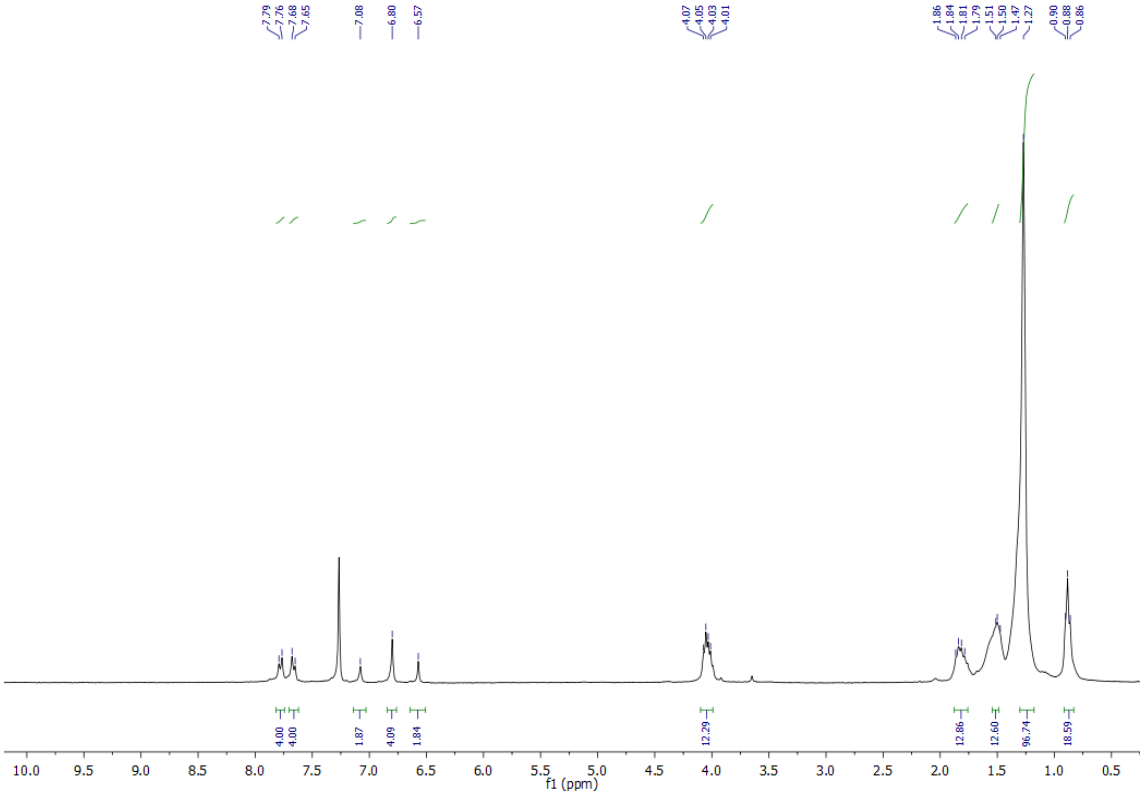

Fig. S3. ^{1}H NMR spectrum of **BDP** in $CDCl_3$.

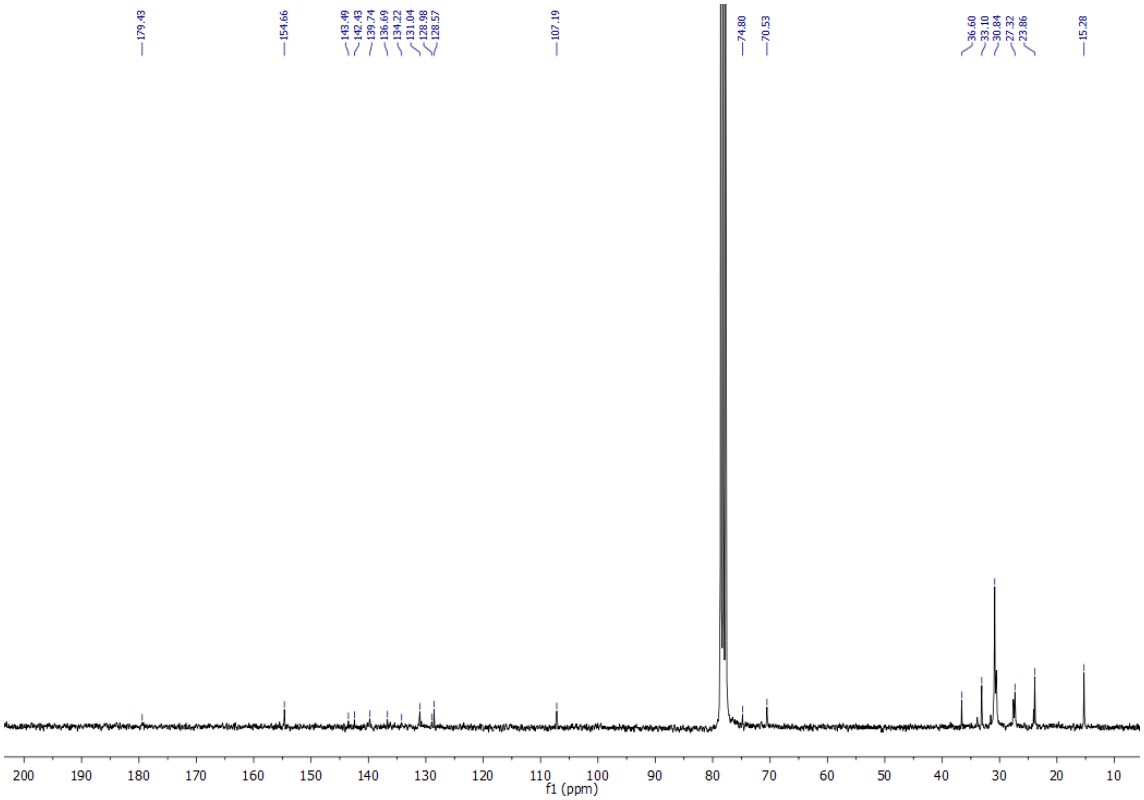

Fig. S4. ^{13}C NMR spectrum of **BDP** in $CDCl_3$.

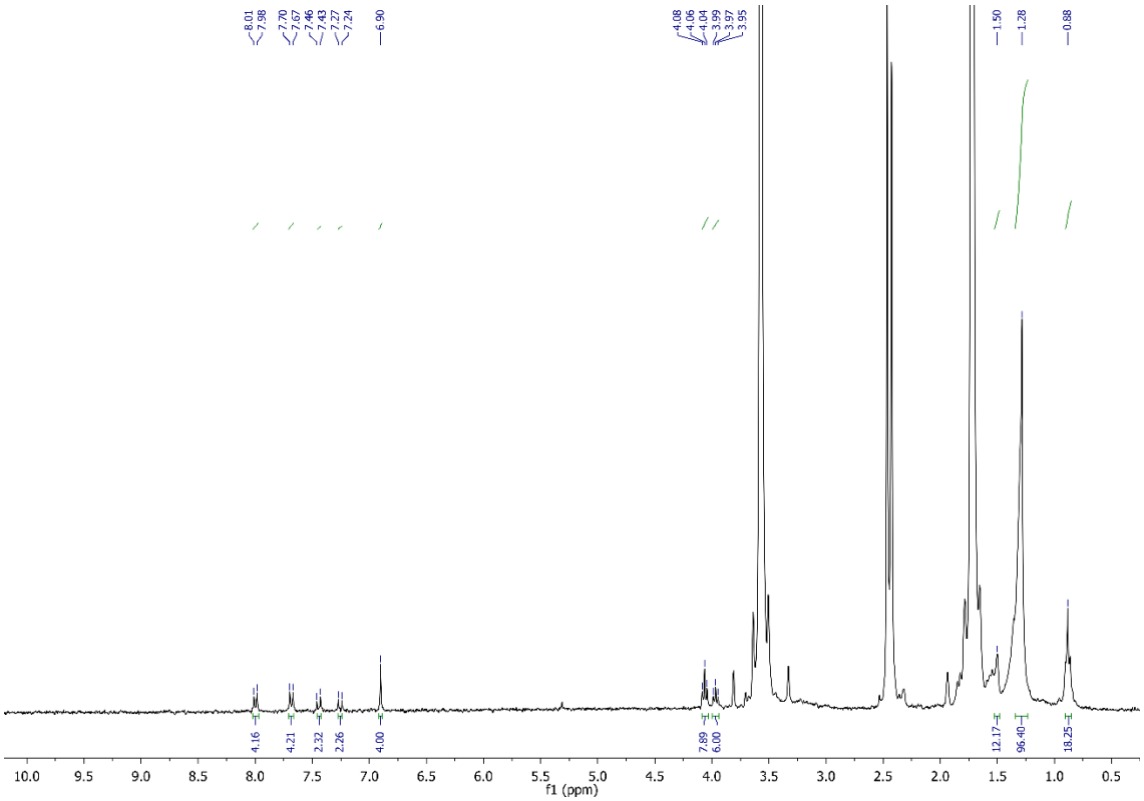

Fig. S5. ^{1}H NMR spectrum of **NDP** in THF-*d8*.

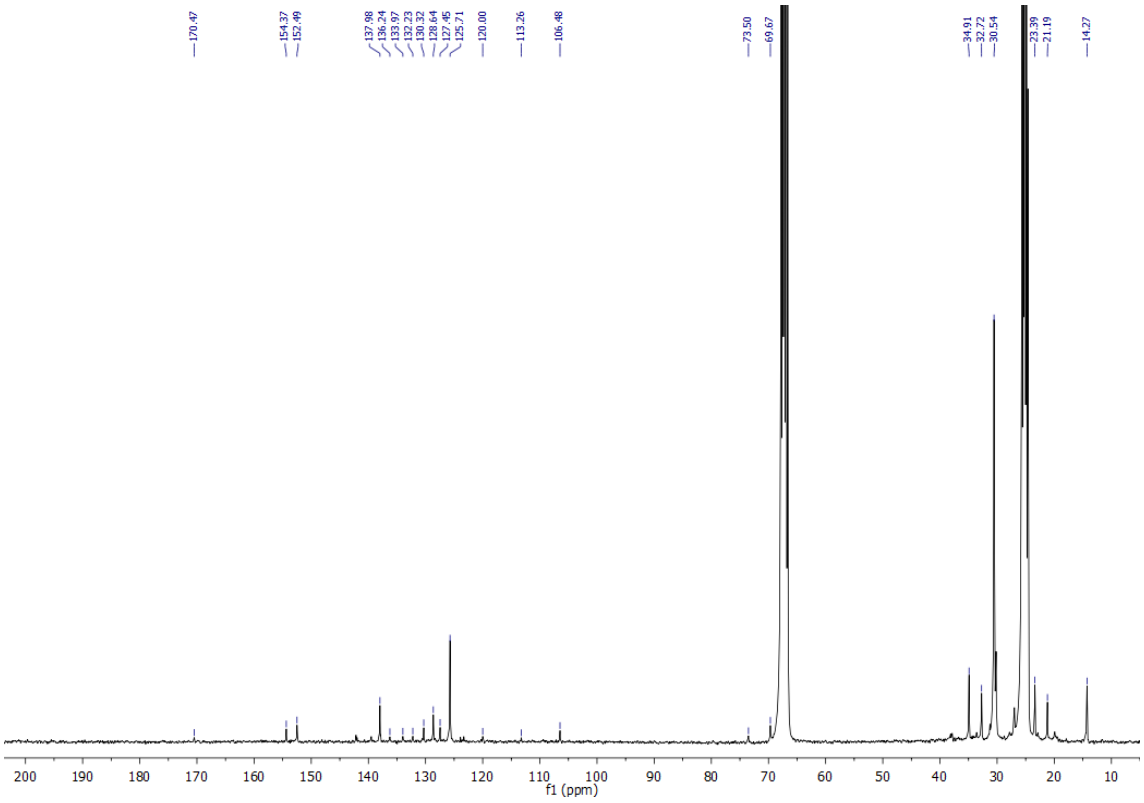

Fig. S6. ^{13}C NMR spectrum of **NDP** in THF-*d8*.

4. Fluorescence studies in solution

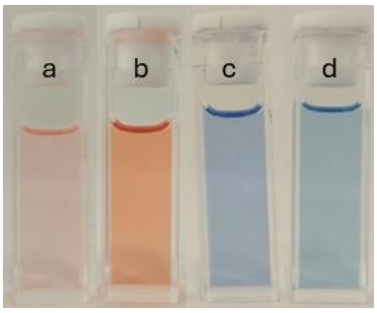

Fig. S7. Photographs of 1×10^{-5} M solutions of **BDP** in (a) chloroform and (b) MCH; and 1×10^{-5} M solutions of **NDP** in (c) chloroform and (d) MCH.

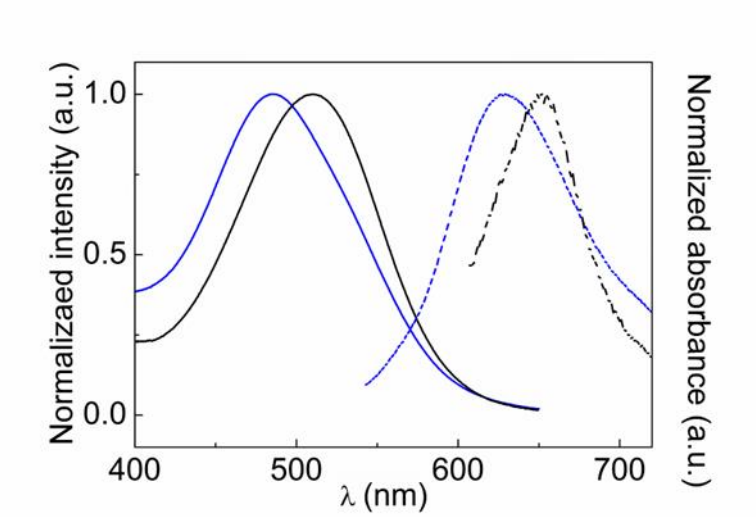

Fig. S8. Normalized emission (dotted lines) and absorption (solid lines) spectra of **BDP** solutions in chloroform (black) and MCH (blue).

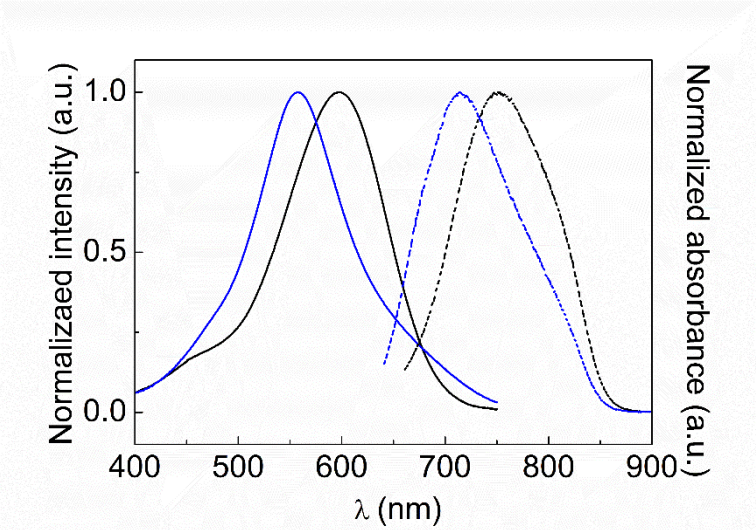

Fig. S9. Normalized emission (dotted lines) and absorption (solid lines) spectra of **NDP** solutions in chloroform (black) and MCH (blue).

5. UV/vis studies in solution

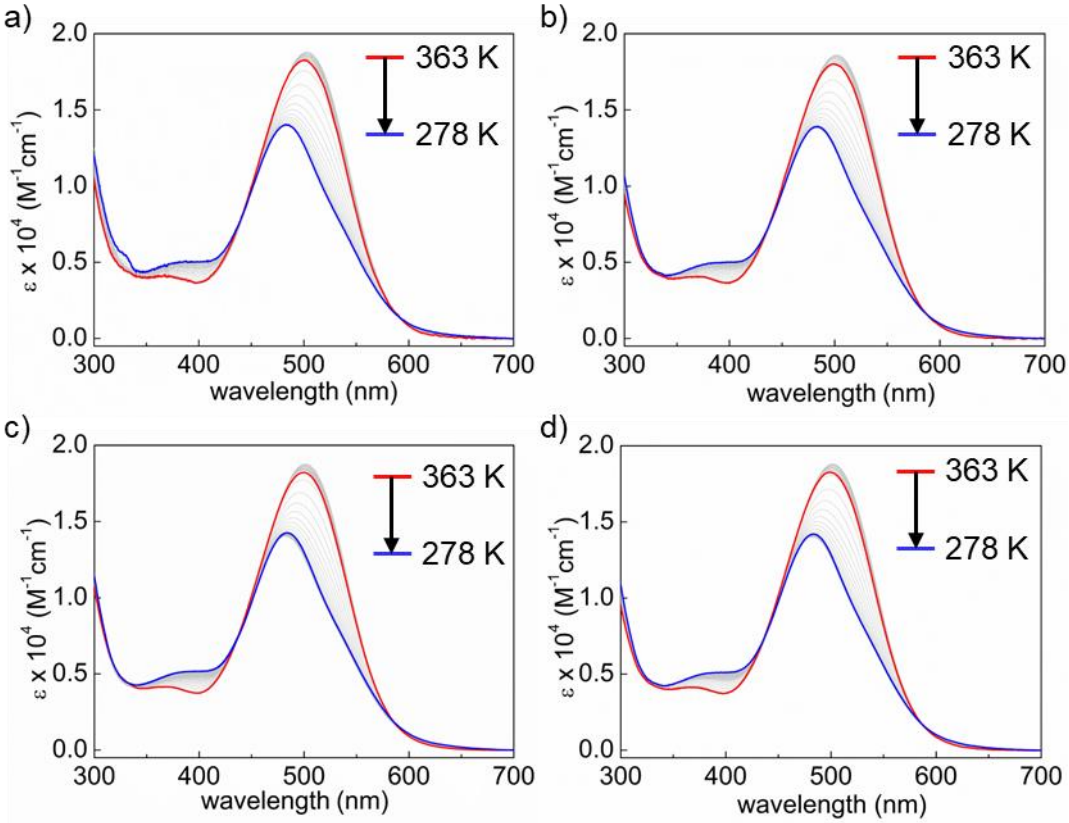

Fig. S10. Temperature-dependent UV/vis experiment of **BDP** solution in MCH from 363 K (red line) to 278 K (blue line) using a cooling rate of 1 K·min^{-1} at different concentrations: (a) 1×10^{-5} M, (b) 2×10^{-5} M, (c) 3×10^{-5} M and (d) 4×10^{-5} M

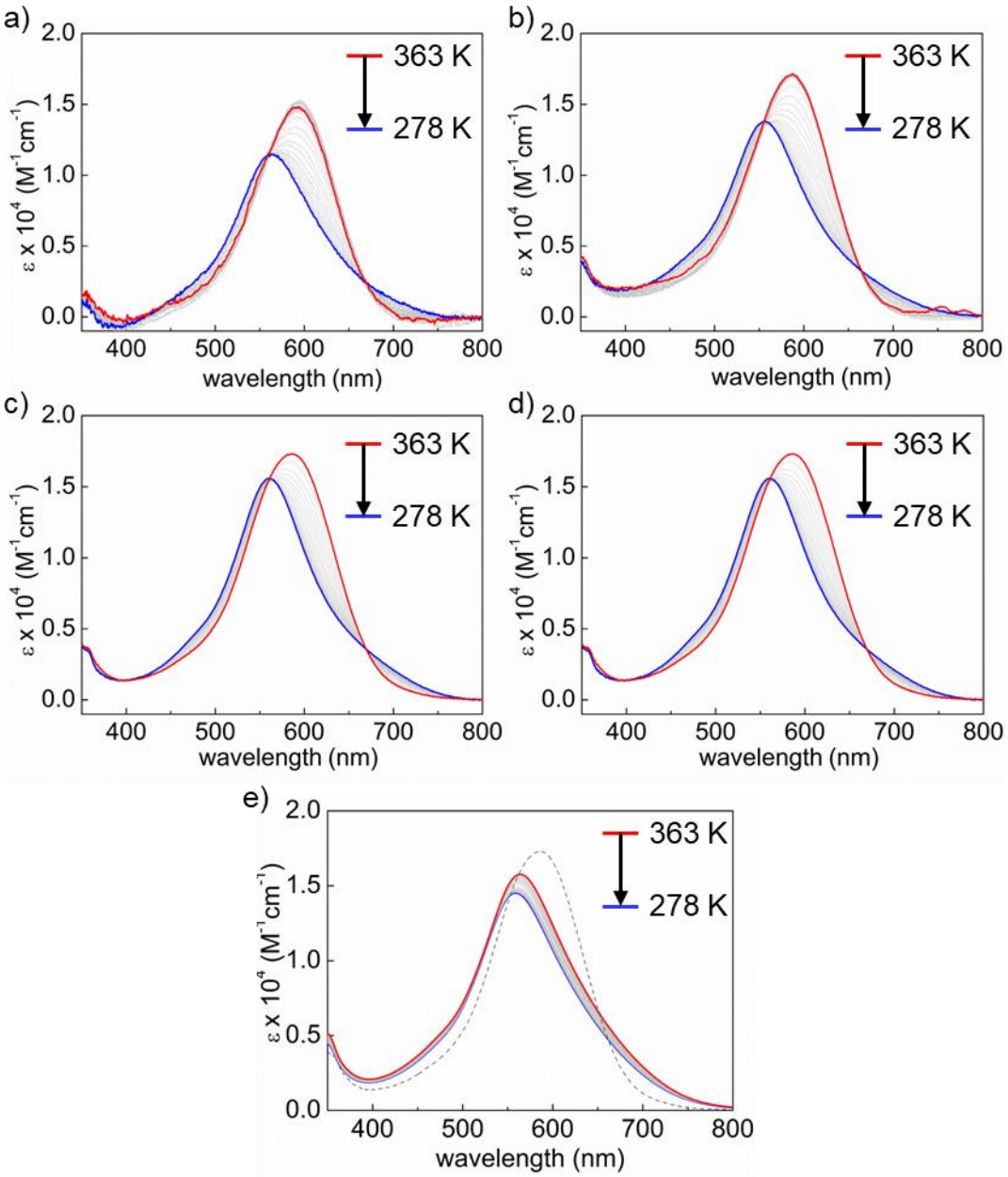

Fig. S11. Temperature-dependent UV/vis experiment of **NDP** solution in MCH from 363 K (red line) to 273 K (blue line) using a cooling rate of 1 K·min^{-1} at different concentrations: (a) 2×10^{-6} M, (b) 5×10^{-6} M, (c) 1×10^{-5} M, (d) 2×10^{-5} M and (e) 5×10^{-4} M. The experiment (e) was carried out in a 1 mm cell to demonstrate the high state of aggregation of the sample, while the temperature control was not accurate. The dashed line represents the spectrum of monomeric **NDP** at 1×10^{-5} M at 363 K.

Nucleation-elongation model for supramolecular polymerizations

BDP and **NDP** compounds forms supramolecular polymer in MCH which are in equilibrium with the monomeric species. The polymerization process can be described with the Nucleation-Elongation Model reported by Ten Eikelder, Markvoort and Meijer.[S4]

The thermodynamic values T_e, $\Delta H°_n$, $\Delta H°$ and $\Delta S°$ can be calculated by a non-linear least-squares analysis of the experimental cooling curves. The equilibrium constants can be calculated by the following equations:

For the nucleation step:

$$K_n = e^{-\frac{(\Delta H° - \Delta H°_n) - T\Delta S°}{RT}}$$

And for the elongation step:

$$K_e = e^{-\frac{\Delta H° - T\Delta S°}{RT}}$$

Finally, the cooperativity factor is obtained by:

$$\sigma = \frac{K_n}{K_e}$$

For a cooperative process $K_n < K_e$ (σ < 1) while for isodesmic process $K_n = K_e$ (σ = 1).

Table S1. Thermodynamic parameters (standard enthalpy ($\Delta H°$), stantard entropy ($\Delta S°$), nucleation enthalpy ($\Delta H°_n$), elongation temperature (T_e), estimated length of the polymer (N), elongation (K_e) and nucleation (K_n) binding constants, and cooperativity factor (σ)) inferred for **BDP** in MCH as solvent at four different concentrations.

Parameter	**BDP** (λ= 482 nm)			
	1×10^{-5} M	2×10^{-5} M	3×10^{-5} M	4×10^{-5} M
$\Delta H°$ (kJ·mol^{-1})	-90.94 ± 0.77			
$\Delta S°$ (J·mol^{-1}·K^{-1})	-0.189 ± 0.003			
$\Delta H°_n$ (kJ·mol^{-1})	-18.31 ± 0.66			
T_e (K)	320.23 ± 0.08	326.86 ± 0.10	330.87 ± 0.12	333.77 ± 0.14
N	101458	51101	33344	24940
$\Delta G°$ (kJ·mol^{-1})	-34.81			
K_e	100630.62	50296.42	33523.59	25138.77
K_n	103.54	59.51	43.04	34.20
σ	1.03×10^{-3}	1.18×10^{-3}	1.28×10^{-3}	1.36×10^{-3}

Table S2. Thermodynamic parameters (standard enthalpy ($\Delta H°$), stantard entropy ($\Delta S°$), nucleation enthalpy ($\Delta H°_n$), elongation temperature (T_e), estimated length of the polymer (N), elongation (K_e) and nucleation (K_n) binding constants, and cooperativity factor (σ)) inferred for **NDP** in MCH as solvent at four different concentrations.

Parameter	**NDP** (λ= 569 nm)			
	2×10^{-6} M	5×10^{-6} M	1×10^{-5} M	2×10^{-5} M
$\Delta H°$ (kJ·mol^{-1})	-95.95 ± 1.32			
$\Delta S°$ (J·mol^{-1}·K^{-1})	-0.177 ± 0.004			
$\Delta H°_n$ (kJ·mol^{-1})	-25.86 ± 4.23			
T_e (K)	335.30 ± 0.21	344.47± 0.21	351.75± 0.26	359.35 ± 0.35
N	532337	212742	106668	52370
$\Delta G°$ (kJ·mol^{-1})	-43.16			
K_e	503551.48	201320.67	100622.56	50292.39
K_n	46.95	24.03	14.48	8.72
σ	9.32×10^{-5}	1.19×10^{-4}	1.44×10^{-4}	1.73×10^{-4}

6. Fourier Transform Infrared Spectroscopy Experiments in solution.

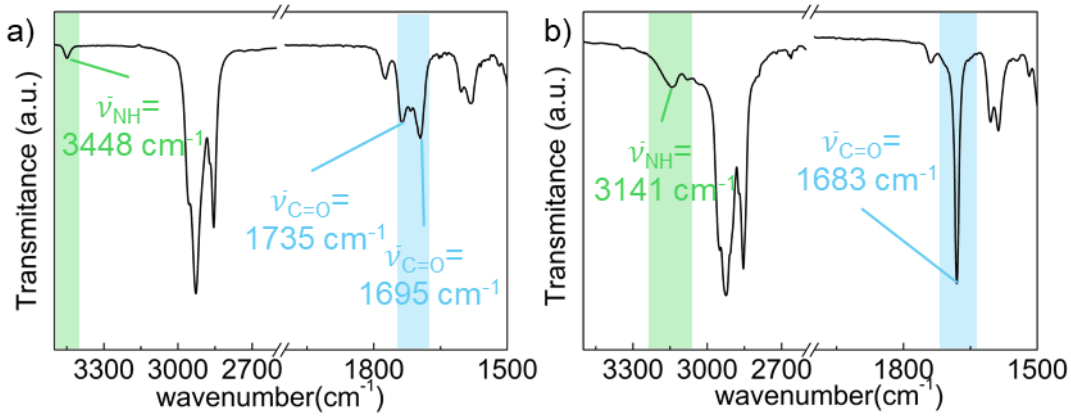

Fig. S12. FT-IR experiment of 1×10^{-3} M **BDP** solution at 25°C in (a) $CDCl_3$ and (b) MCH-*d14*

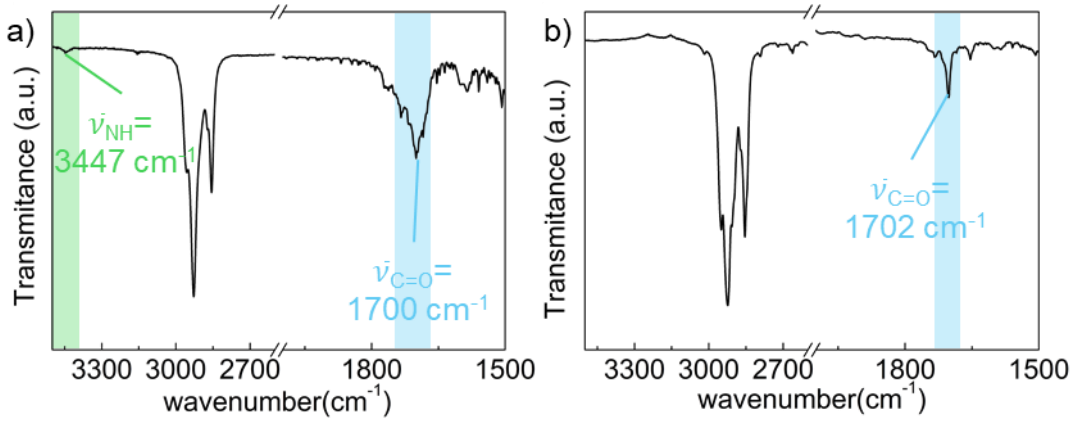

Fig. S13. FT-IR experiment of 1×10^{-3} M **NDP** solution at 25°C in (a) $CDCl_3$ and (b) MCH-*d14*

7. Competitive UV-Vis studies in solution.

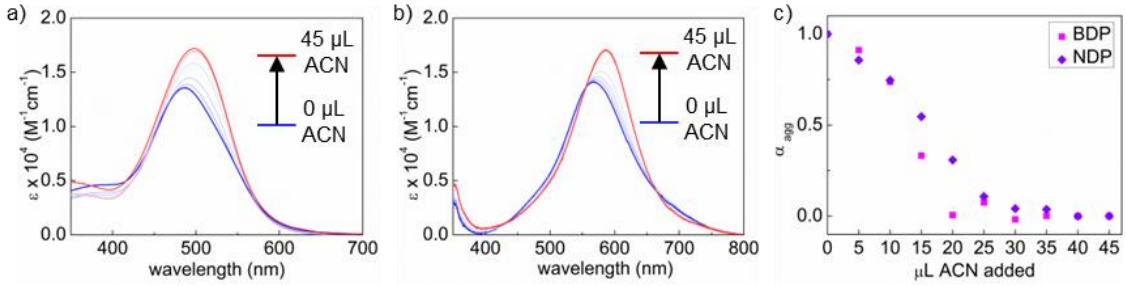

Fig. S14. UV-Vis spectra of a) **BDP** (MCH, 1 x 10^{-5} M) and b) **NDP** (MCH, 1 x 10^{-5} M) after increasing additions of ACN (5µL). In blue is represented the aggregated species and in red the monomeric states. After the addition of more than 45 µL the solvents show no miscibility. c) Representation of the α_{agg} of **BDP** (pink squares) and **NDP** (purple diamonds) as a function of the added volume of ACN.

8. NMR temperature dependant experiments.

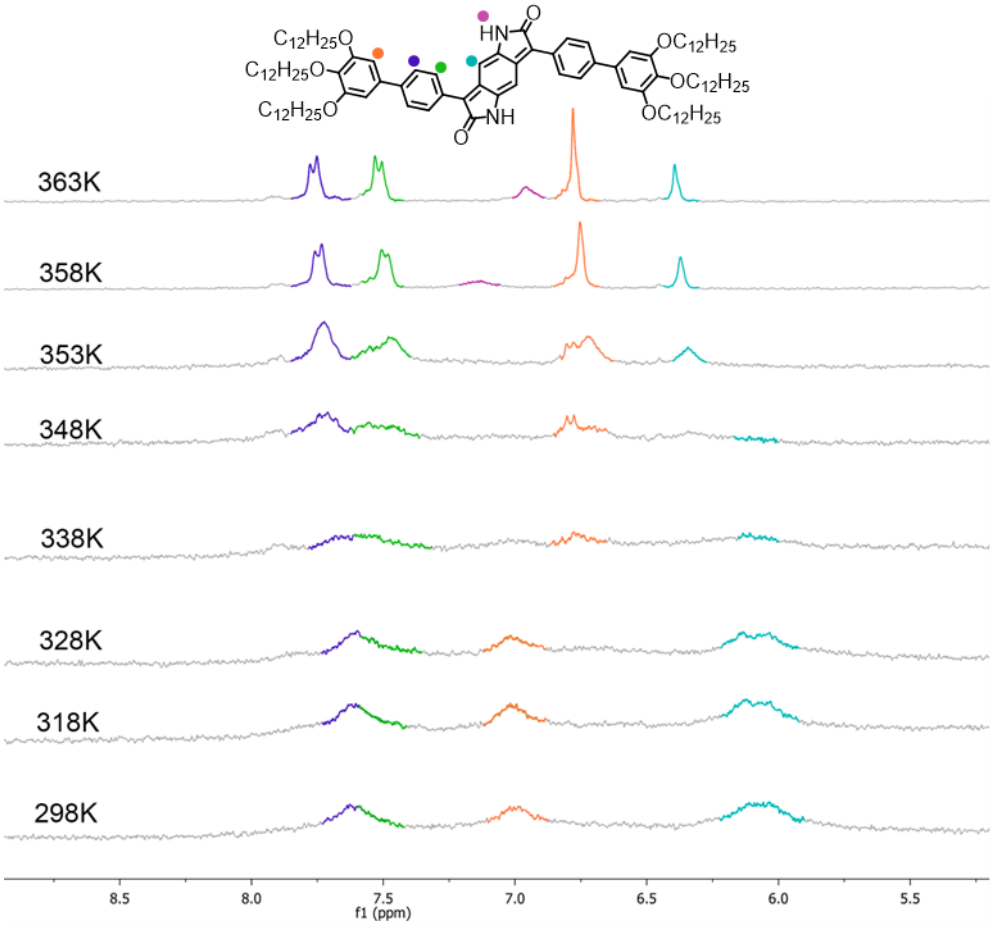

Fig. S15. ^{1}H NMR spectra **BDP** in MCH-*d14* (5×10^{-4} M) at different temperatures.

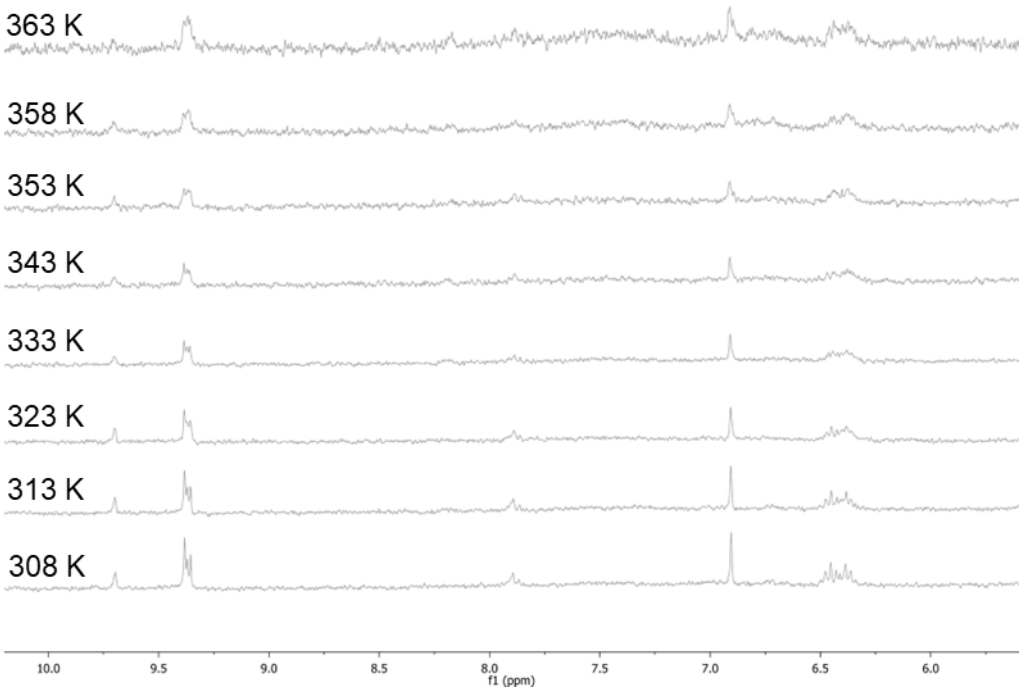

Fig. S16. ^{1}H NMR spectra of **NDP** in MCH-*d14* (5×10^{-4} M) at different temperatures.

9. Morphology studies of the supramolecular polymers.

Sample preparation

50 µL of a previously prepared 4×10^{-5} M of **BDP** in MCH were spin-coated onto mica and high oriented pyrolytic graphite (HOPG) surface. Then, both surfaces were dried with a nitrogen flux for 5 min.

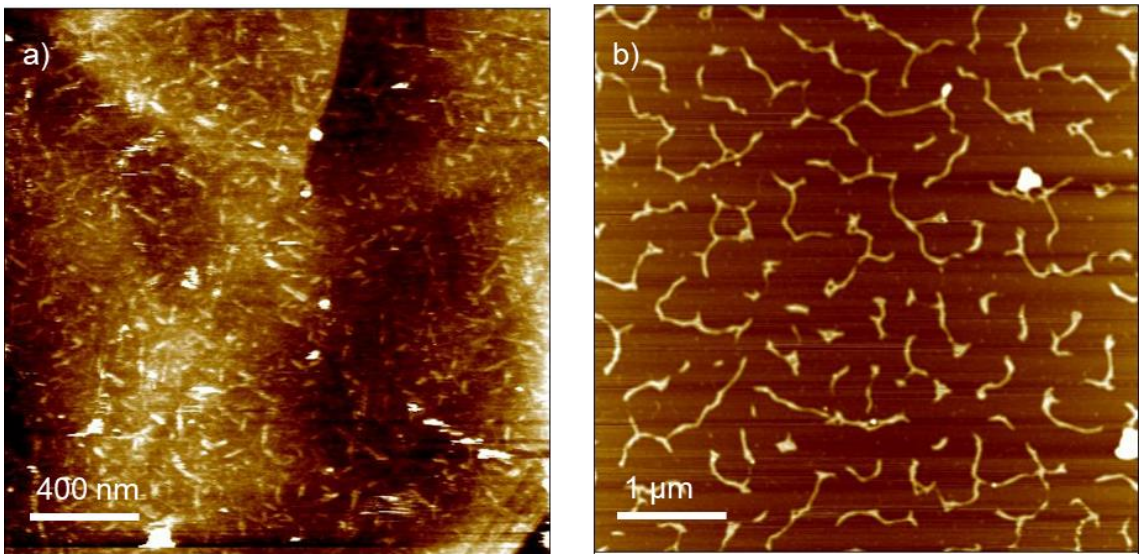

Fig. S17. Atomic force microscopy image of a spin-coated solution of **BDP** in MCH (4×10^{-5} M) on HOPG (a) and mica (b) surface.

Sample preparation

50 µL of a previously prepared 4×10^{-5} M of **NDP** in MCH were spin-coated onto HOPG. surface. Then, the surface was dried with a nitrogen flux for 5 min.

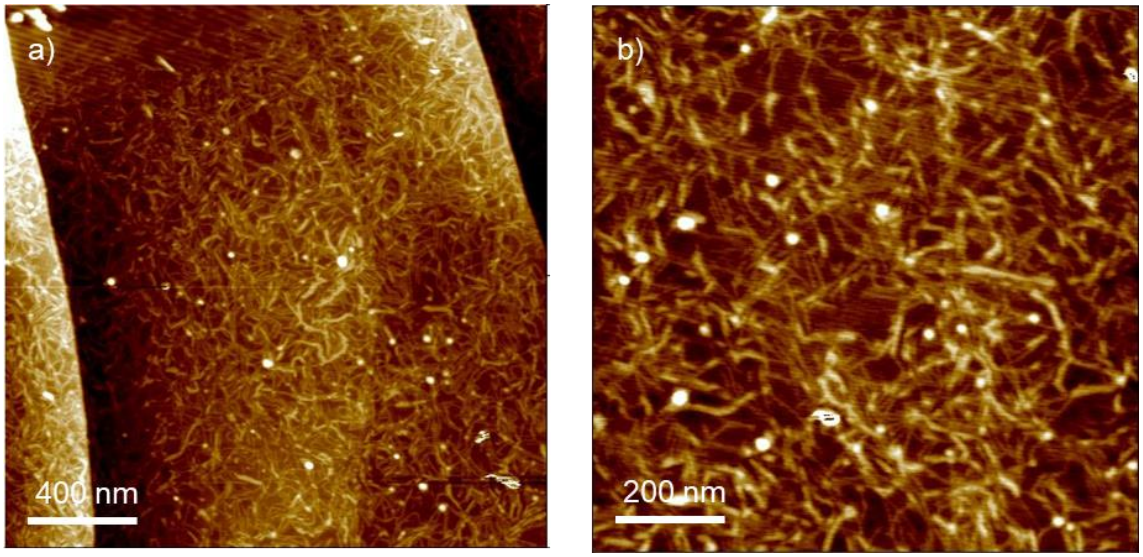

Fig. S18. (a) and (b) Atomic force microscopy image of a spin-coated solution of **NDP** in MCH (4×10^{-5} M) on HOPG surface.

10. Polarizing Optical microscope studies

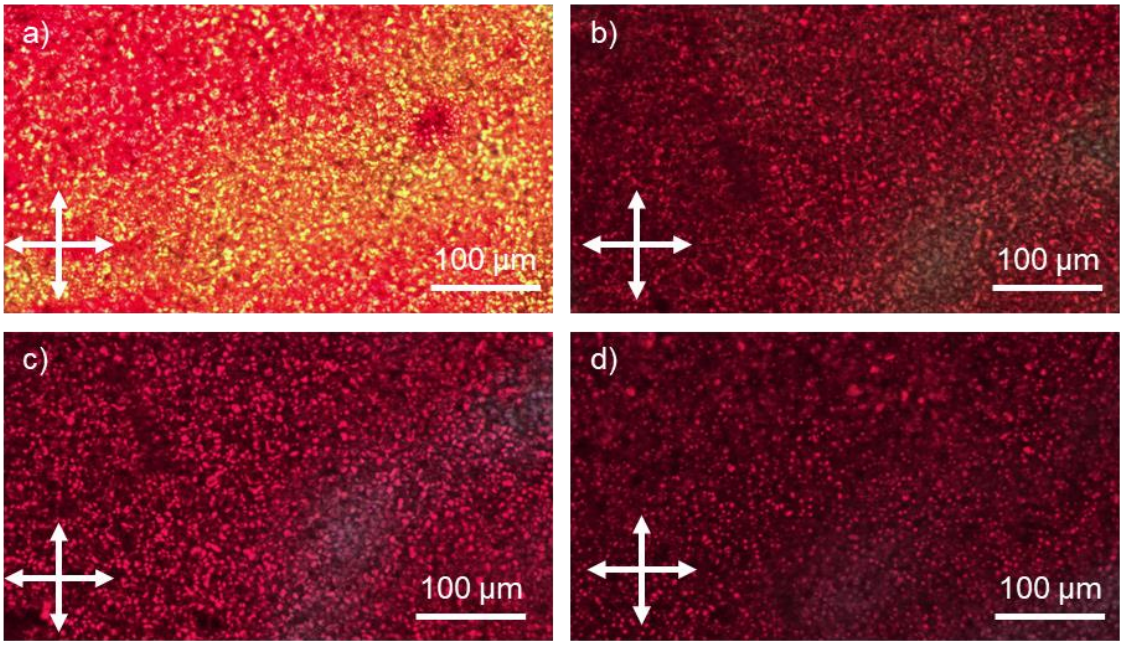

Fig. S19. Polarized optical microscopic images of **BDP** at (a) 180°C, (b) 120°C, (c) 50°C and (d) 25°C.

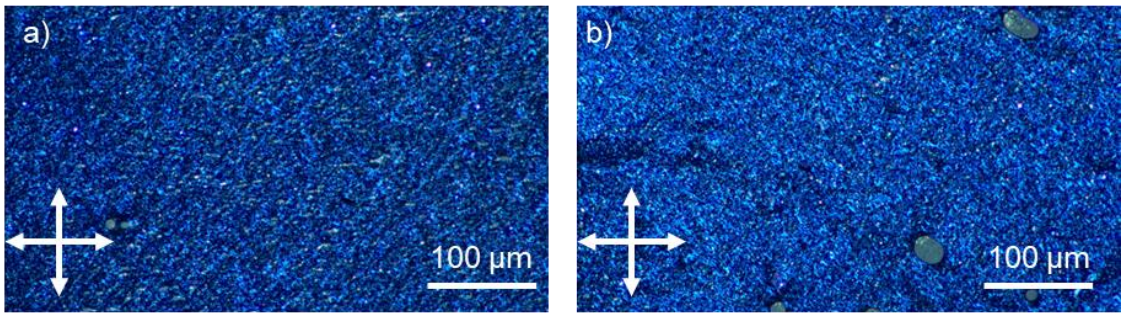

Fig. S20. Polarized optical microscopic images of **NDP** at (a) 150°C and (b) 25°C

11. DSC experiments

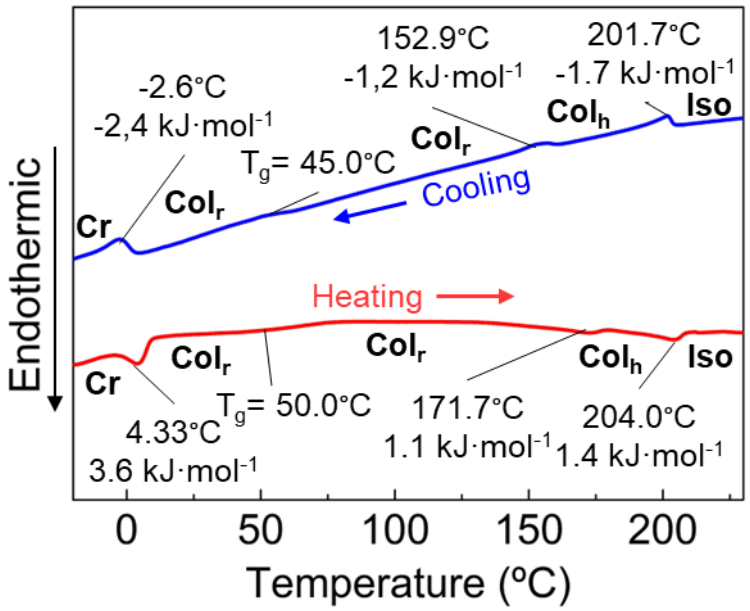

Fig. S21. Differential scanning calorimetry traces on a first cooling (blue line) and second heating (red line) of **BDP**. Heating/cooling rate 10°C·min^{-1}. Transition temperatures indicated correspond to the onset values.

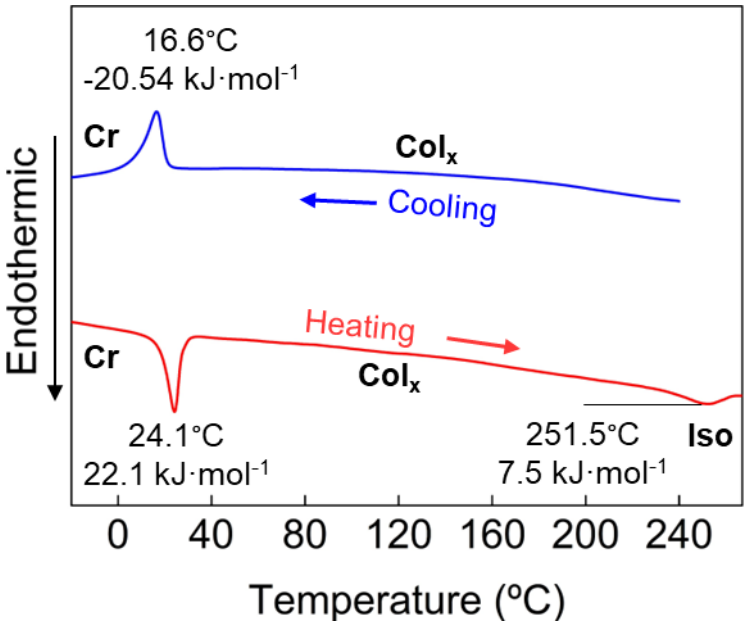

Fig. S22. Differential scanning calorimetry traces on a first cooling (blue line) and second heating (red line) of **NDP**. Heating/cooling rate 10°C·min^{-1}. First heating was until 240°C to avoid decomposition of the product when it goes to Isotropic phase. Transition temperatures indicated correspond to the onset values.

12. X-ray studies

Sample preparation

Analysis of the samples were in a fibrillar form. To obtain the fibres we used a home-made extruder. We introduced the sample into the extruder and then with the metallic bar we made pressure downwards to obtain the fibre of 0.8-1.2 mm of diameter.

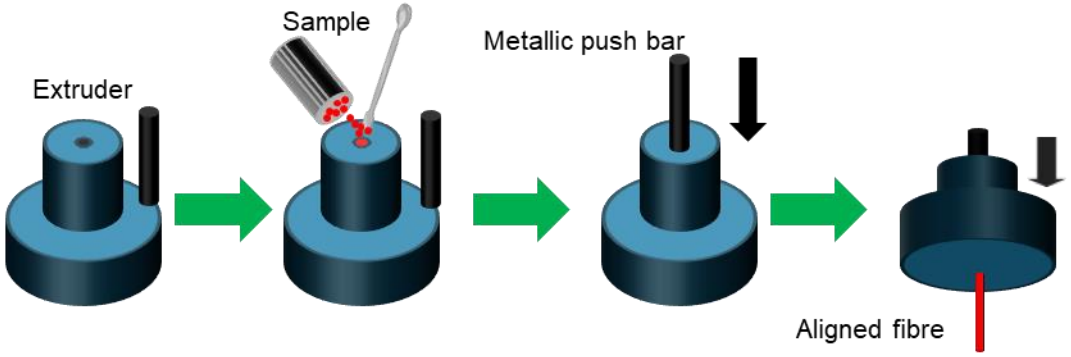

Fig. S23. Scheme of the preparation of aligned fibers of the liquid crystals using a homemade extruder.

Data analysis

The X-ray data was analyzed using the Datasqueeze 3.0 Software.[S5]

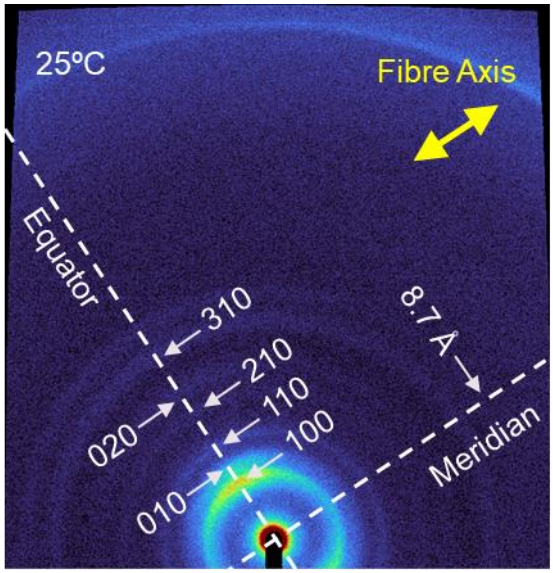

Fig. S24. 2D WAXS pattern of an aligned fibre of **BDP** at 25 °C.

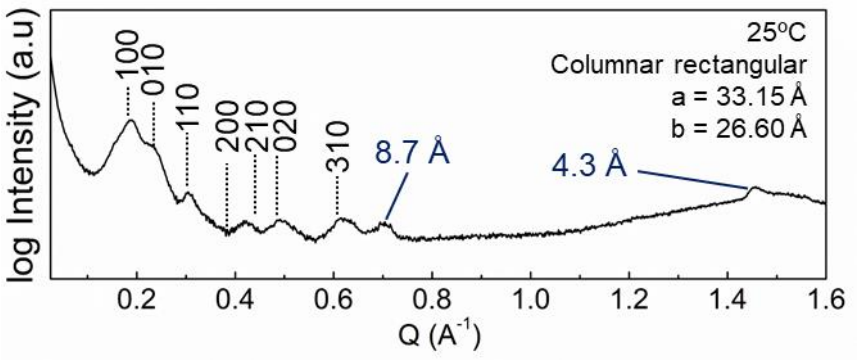

Fig. S25 Integrated intensities along the equator of the WAXS pattern of **BDP** at 25 °C, showing the reflections indexed according to the columnar rectangular assembly.

Table S3. Data of the equator of the WAXS pattern of **BDP** at 25 °C. comparing to the theoretical columnar rectangular geometry reflections.

Entry	hkl	d_{exp} / Å	d_{calc} / Å	Δ / Å
1	100	33.1	33.2	0.1
2	010	26.7	26.6	0.1
3	110	20.8	20.8	0.0
4	200	16.6	16.6	0.0
5	210	14.1	14.0	0.1
6	020	13.3	13.3	0.0
7	310	10.2	10.2	0.0

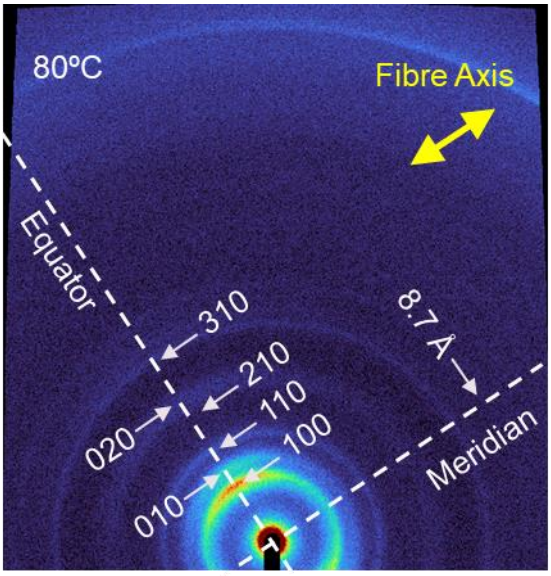

Fig. S26. 2D WAXS pattern of an aligned fibre of **BDP** at 80 °C.

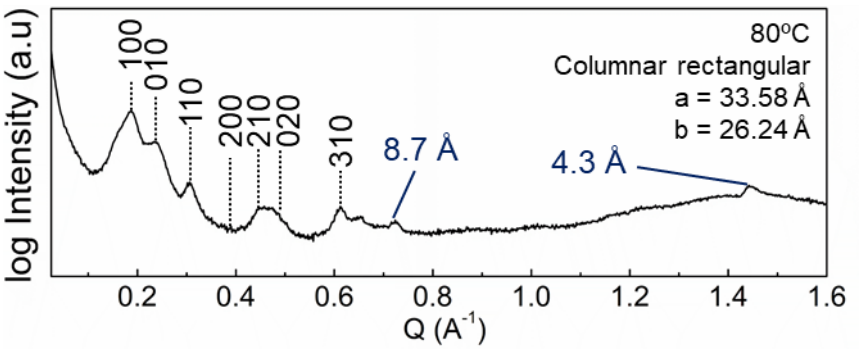

Fig. S27. Integrated intensities along the equator of the WAXS pattern of **BDP** at 80 °C, showing the reflections indexed according to the columnar rectangular assembly.

Table S4. Data of the equator of the WAXS pattern of **BDP** at 80 °C. comparing to the theoretical columnar rectangular geometry reflections.

Entry	hkl	d_{exp} / Å	d_{calc} / Å	Δ / Å
1	100	33.6	33.6	0.0
2	010	26.2	26.2	0.0
3	110	20.6	20.7	0.1
4	200	16.9	16.8	0.1
5	210	13.9	14.1	0.2
6	020	13.3	13.1	0.2
7	310	11.2	11.2	0.0

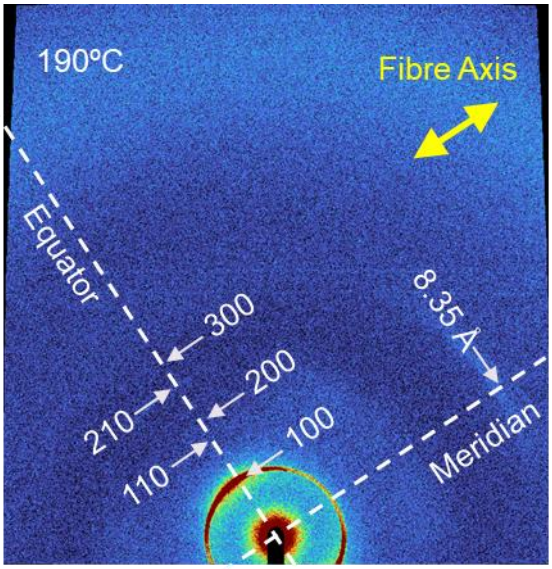

Fig. S28. 2D WAXS pattern of an aligned fibre of **BDP** at 190 °C.

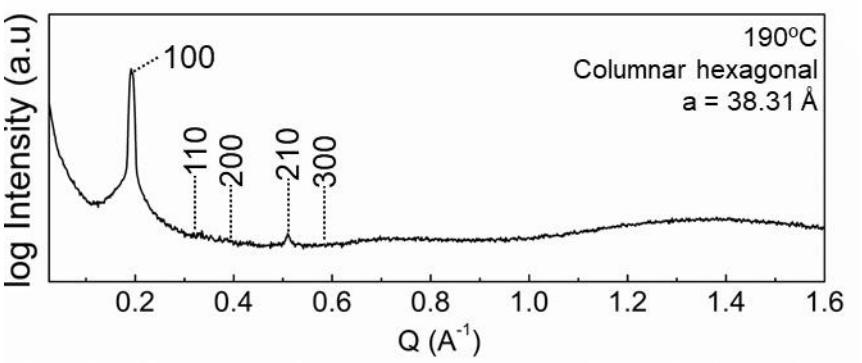

Fig. S29. Integrated intensities along the equator of the WAXS pattern of **BDP** at 190 °C, showing the reflections indexed according to the columnar hexagonal assembly.

Table S5. Data of the equator of the WAXS pattern of **BDP** at 190 °C. comparing to the theoretical columnar hexagonal geometry reflections.

Entry	hkl	d_{exp} / Å	d_{calc} / Å	Δ / Å
1	100	33.2	33.2	0.0
2	110	19.1	19.2	0.1
3	200	16.9	16.6	0.3
4	210	12.6	12.5	0.1
5	300	11.3	11.1	0.2

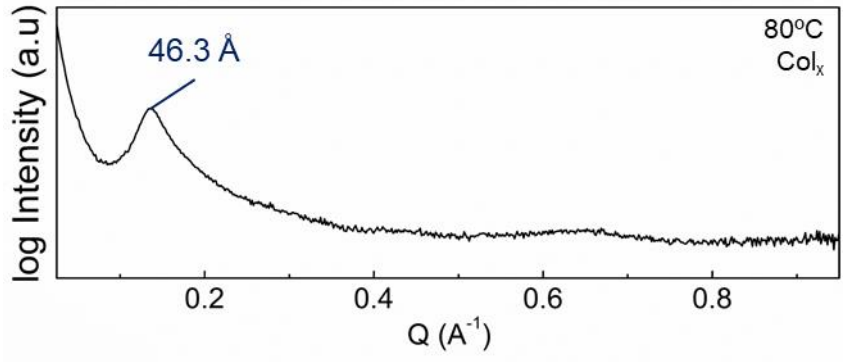

Fig. S30. Integrated intensities along the equator of the WAXS pattern of **NDP** at 80 °C.

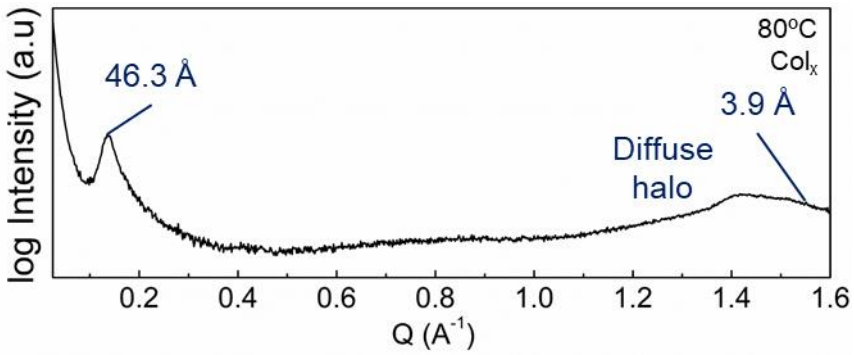

Fig. S31. Integrated intensities along the meridian of the WAXS pattern of **NDP** at 80 °C.

Calculation of the number of molecules per columnar stratum

The number of molecules per unit cell of the columnar phases of compound **BDP** and **NDP** were calculated using the parameters obtained from the WAXS patterns and the following equations: [S6-7]

$$V_{unit\ cell} = a \times b \times c \times sen(\gamma)$$

$$Z = \frac{\delta \times N_A \times V_{unit\ cell}}{M}$$

a, b, c = unit cell parameter
ɣ = angle between the two directors of the unit cell
Z = number of mollecules per unit cell
δ = density
M = molecular mass
N_A = Avogadro's Number
$V_{unit\ cell}$ = unit cell volume

Table S6. Parameters extracted from the WAXS pattern of **BDP** at 25 °C for the calculation of the number of molecules per unit cell.

Parameter	Value
a	33.15 Å
b	26.60 Å
c	8.7 Å
ɣ	90º
M	1.59650 kg/mol
δ	1000 kg/m^3 (supposed)
NA	6.022·10^{23} mol^{-1}
V_{unitcell}	7671.6 Å^3 = 7.67·10^{-27} m^3
Z	2.89 ≈ 3

Table S7. Parameters extracted from the WAXS pattern of **BDP** at 80 °C for the calculation of the number of molecules per unit cell.

Parameter	Value
a	33.58 Å
b	26.24 Å
c	8.7 Å
ɣ	90º
M	1.59650 kg/mol
δ	1000 kg/m^3 (supposed)
NA	6.022·10^{23} mol^{-1}
V_{unitcell}	7665.9 Å^3 = 7.67·10^{-27} m^3
Z	2.89 ≈ 3

Table S8. Parameters extracted from the WAXS pattern of **BDP** at 190 °C for the calculation of the number of molecules per unit cell.

Parameter	Value
a	38.31 Å
b	38.31 Å
c	8.35 Å
ɣ	120 ^{o}
M	1.59650 kg/mol
δ	1000 kg/m^3 (supposed)
NA	6.022·10^{23} mol^{-1}
V_{unitcell}	10613.1 Å^3 = 1.061·10^{-26} m^3
Z	4.00 ≈ 4

13. Anisotropic experiments in solid state

Polarized UV/vis spectroscopy experiments

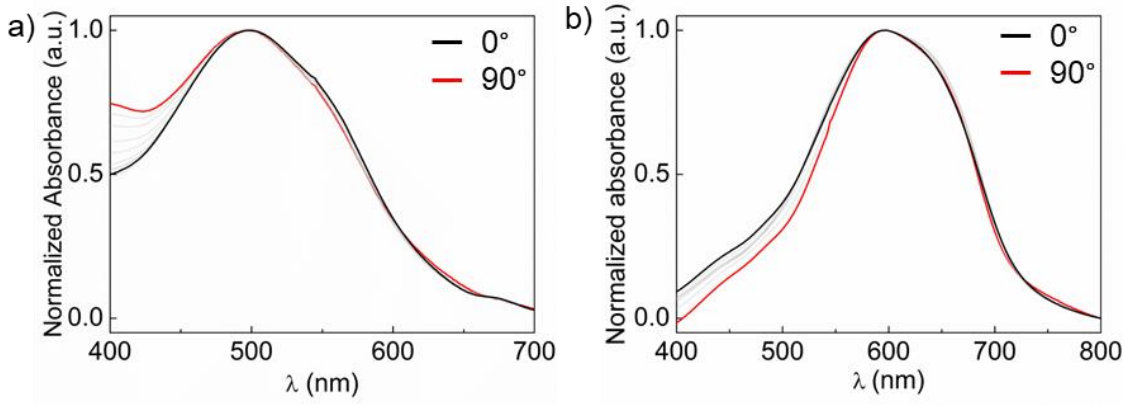

Fig. S32. Polarized UV/vis spectra of aligned samples (mechanical shearing) of (a) **BDP** and (b) **NDP** on a quartz plate acquired with the polarizer parallel (red) and perpendicular (black) to the shearing direction.

Polarizing Optical microscope studies

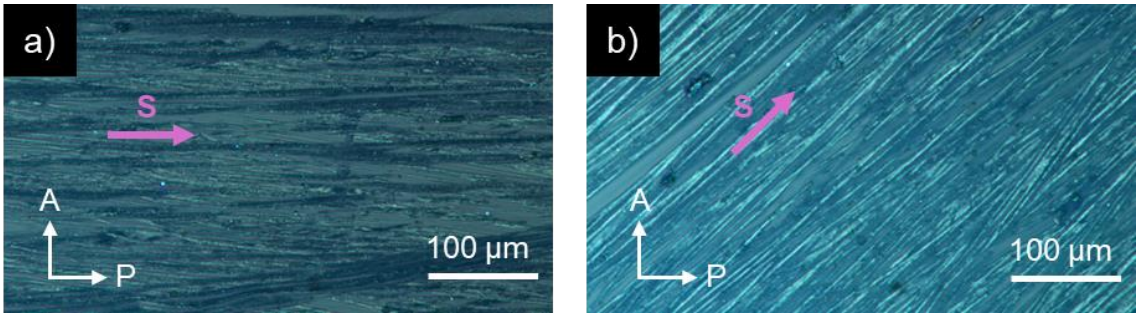

Fig. S33. Polarized optical microscopic images of **NDP** after mechanical shearing with the Polarizer (P) (a) parallel to the shearing direction and (b) after sample holder rotation of 45°.

Polarized Fourier Transform Infrared Spectroscopy experiments

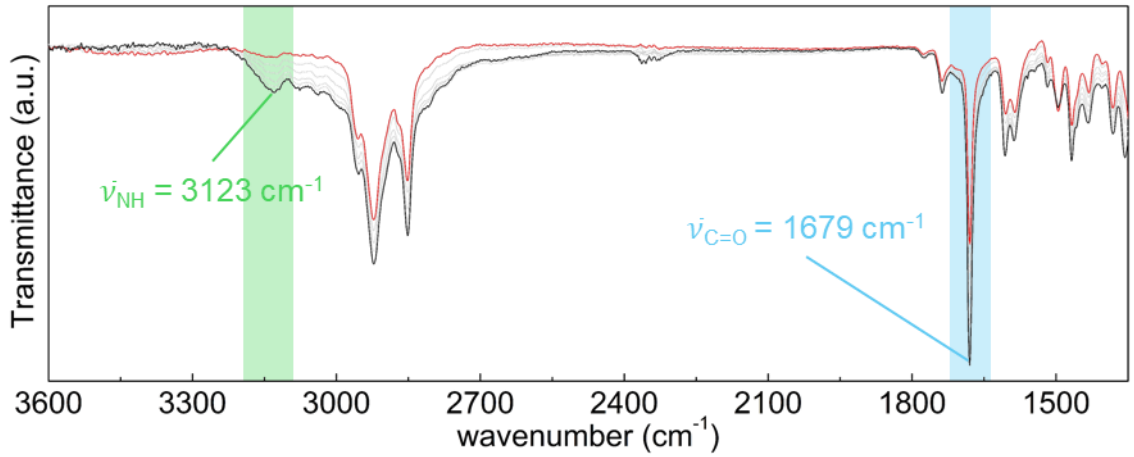

Fig. S34. Polarized Fourier Transform Infrared spectra of an aligned sample (mechanical shearing) of **BDP** on a KBr pellet acquired with the polarizer parallel (red) and perpendicular (black) to the shearing direction.

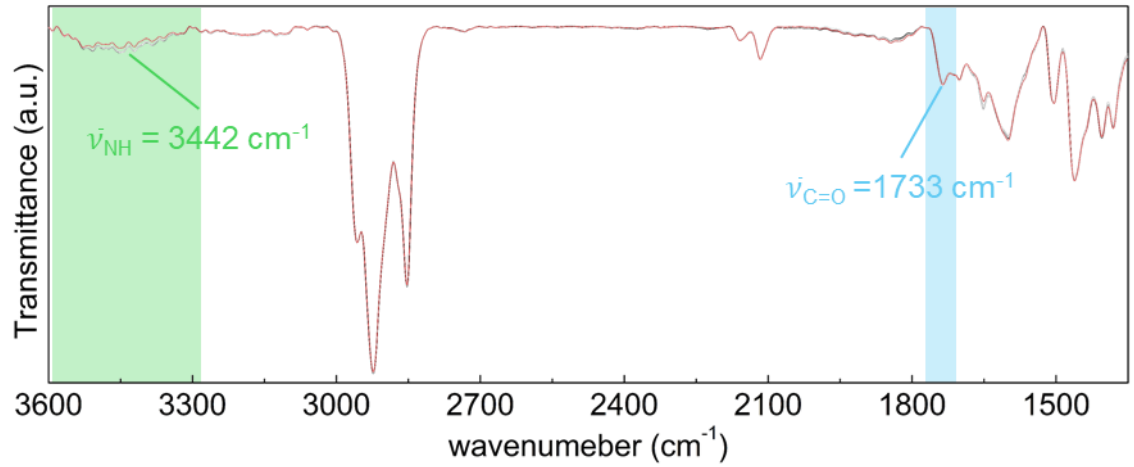

Fig. S35. Polarized Fourier Transform Infrared spectra of an aligned sample (mechanical shearing) of **NDP** on a KBr pellet acquired with the polarizer parallel (red) and perpendicular (black) to the shearing direction.

14. References

S1. H. Maeda, K. Chigusa, T. Sakurai, K. Ohta, S. Uemura, S. Seki, Ion-Pair-Based Assemblies Comprising Pyrrole–Pyrazole Hybrids, *Chem. Eur. J.*, 2013, **19**, 9224–9233.

S2. W. Cui, J. Yuen, F. Wudl, Benzodipyrrolidones and their polymers, *Macromolecules*, 2011, **44**, 7869–7873.

S3. H. Zhang, K. Yang, Y. Chen, R. Bhatta, M. Tsige, S. Z. Cheng, Y. Zhu, Polymers Based on Benzodipyrrolidone and Naphthodipyrrolidone with Latent Hydrogen-Bonding on the Main Chain, *Macromol. Chem. Phys.*, 2017, **218**, 1600617.

S4. A. J. Markvoort, H. M. M. ten Eikelder, P. A. J. Hilbers, T. F. A. de Greef and E. W. Meijer, Theoretical models of nonlinear effects in two-component cooperative supramolecular copolymerizations, *Nat. Commun.,* 2011, **2**, 509.

S5. P. A. Heiney, 2D Powder Diffraction, *IUCR Commission on Powder Diffraction Newsletter,* 2005, **32**, 9-11.

S6. N. Godberg, A. Crispini, M. Ghedini, M. Carini, F. Chiaravalloti and A. Ferrise, LCDiXRay: a user-friendly program for powder diffraction indexing of columnar liquid crystals, J. *Appl. Crystallogr.,* 2014, **47**, 668-679.

S7. D. Sahoo, M. Peterca, E. Aqad, B. E. Partridge, P. A. Heiney, R. Graf, H. W. Spiess, X. Zeng and V. Percec, Hierarchical Self-Organization of Perylene Bisimides into Supramolecular Spheres and Periodic Arrays Thereof, *J. Am. Chem. Soc.,* 2016, **138**, 14798-14807.